The luminosity function and surface brightness distribution of HI selected galaxies

Zwaan, Martin A.; Briggs, Frank H.; Sprayberry, David

Published in:
Monthly Notices of the Royal Astronomical Society

DOI:
10.1046/j.1365-8711.2001.04844.x

Publication date:
2001

Mon. Not. R. Astron. Soc. **327,** 1249–1259 (2001)

The luminosity function and surface brightness distribution of H I selected galaxies

Martin A. Zwaan,[1,2]★ Frank H. Briggs[2] and David Sprayberry[3]

[1]*Astrophysics Group, School of Physics, University of Melbourne, Victoria 3010, Australia*
[2]*Kapteyn Astronomical Institute, P.O. Box 800, 9700 AV Groningen, the Netherlands*
[3]*W. M. Keck Observatory, 65-1120 Mamalahoa Highway, Kamuela, HI 96743, USA*

Accepted 2001 July 9. Received 2001 July 9; in original form 2001 May 18

ABSTRACT

We measure the $z = 0$ B-band optical luminosity function (LF) for galaxies selected in a blind H I survey. The total LF of the H I selected sample is flat, with Schechter parameters $M^* = -19.38^{+1.02}_{-0.62} + 5\log h_{100}$ mag and $\alpha = -1.03^{+0.25}_{-0.15}$, in good agreement with LFs of optically selected late-type galaxies. Bivariate distribution functions of several galaxy parameters show that the H I density in the local Universe is more widely spread over galaxies of different size, central surface brightness and luminosity than the optical luminosity density is. The number density of very low surface brightness (LSB) (>24.0 mag arcsec^{-2}) gas-rich galaxies is considerably lower than that found in optical surveys designed to detect dim galaxies. This suggests that only a part of the population of LSB galaxies is gas-rich and that the rest must be gas-poor. However, we show that this gas-poor population must be cosmologically insignificant in baryon content. The contribution of gas-rich LSB galaxies (>23.0 mag arcsec^{-2}) to the local cosmological gas and luminosity density is modest (18^{+6}_{-5} and 5^{+2}_{-2} per cent respectively); their contribution to $\Omega_{\rm matter}$ is not well-determined, but probably <11 per cent. These values are in excellent agreement with the low redshift results from the Hubble Deep Field.

Key words: galaxies: fundamental parameters – galaxies: luminosity function, mass function – galaxies: statistics.

1 INTRODUCTION

Understanding galaxy evolution requires well-determined local benchmarks. One of the most fundamental of these is the field galaxy luminosity function, the shape of which should be predicted by any reliable galaxy formation theory. In principle, the shape of the luminosity function is related to the power spectrum of primordial density fluctuations and complex processes such as gas cooling, star formation and feedback to the interstellar medium, as well as the behaviour of dark matter as it undergoes gravitational collapse and merging in galaxy halos (see e.g. Cole et al. 2000 for a recent review). Reference points in the local Universe will help in developing a full understanding of these processes. Another motive for the determination of the local luminosity function is the problem of the faint blue galaxies. The normalization of the $z = 0$ luminosity function seems to be too low to be reconciled with no-evolution predictions based on intermediate redshift ($z \sim 1$) surveys (Ellis 1997; Broadhurst, Ellis & Shanks 1988; Koo & Kron 1992), but to quantify this problem a reliable measurement of the faint-end slope is essential.

The last few years have seen a proliferation of published luminosity functions from optical redshift surveys of the local ($z < 0.2$) Universe (see e.g. Zucca et al. 1997; Ratcliffe et al. 1998; Folkes et al. 1999; also Blanton et al. 2001 for some recent examples). These surveys systematically produce samples of 10^4 galaxies and are able to determine the luminosity function down to absolute magnitude limits of $M_B = -14$. However, considerable uncertainty remains about the exact shape and normalization of the luminosity function. Especially the faint-end slope for the dwarf galaxies ($M_B > -18$) is practically unconstrained (see discussion in Driver & Phillipps 1996).

A potential cause of the uncertainty in low-z galaxy counts is the surface brightness selection effect (Disney 1976; Disney & Phillips 1987). Sprayberry et al. (1997) specifically searched for the low surface brightness (LSB) galaxies in the APM survey (Impey et al. 1996), and concluded that including LSB galaxies in the low-z census steepens the field luminosity function, but still does not close the gap between number counts at moderate redshift and $z = 0$.

The discussion on LSB galaxies ties in directly with another important benchmark at $z = 0$: the distribution function of optical surface brightnesses. Based on photometry of 36 nearby spiral and

★E-mail: mazwaan@unimelb.edu.au

S0 galaxies, Freeman (1970) concluded that ~80 per cent have a B-band central surface brightness $\mu_B(0)$ in the range 21.65 ± 0.30 mag arcsec^{-2}. The eight deviant galaxies consisted of one dwarf irregular LSB galaxy [$\mu_B(0) = 23.7$ mag arcsec^{-2}] and seven brighter galaxies of various morphological type. The majority opinion at the present moment seems to be that the distribution function is flat (McGaugh 1996; de Jong 1996; Dalcanton et al. 1997b; O'Neil & Bothun 2000; de Jong & Lacey 2000; Blanton et al. 2001; Cross et al. 2001), although Sprayberry, Impey & Irwin (1996) found a distribution function that peaks at ~22 mag arcsec^{-2}. Tully & Verheijen (1997) have a dissenting view and present evidence for bimodality in the distribution of near-infrared surface brightnesses in the Ursa Major Cluster. This view has been contested by Bell & de Blok (2000) who claim that the data set is insufficient to establish the presence of a bimodal surface brightness distribution.

New insight into both issues can be obtained by selecting galaxies via a method that is free from optical selection effects. In this paper we measure for the first time the optical luminosity function and surface brightness distribution function of H I selected galaxies. This sample is the result of the Arecibo H I Strip Survey, a blind strip survey in the 21-cm line. We stress that this sample is small (60 members) compared to those produced by modern redshift surveys, and large statistical errors are therefore unavoidable. This work should be regarded as the first step toward measuring these functions for H I selected galaxy samples. Much larger galaxy samples will be available in the near future (e.g. HIPASS, Staveley-Smith et al. 1996), and the measurements of optical luminosity functions, surface brightness functions and bivariate distributions will greatly improve.

We organize this paper as follows. First, in Section 2, we briefly describe the sample. In Section 3 we present the optical luminosity function of this H I selected galaxy sample, and discuss the distribution of luminosity density and H I gas density among different galaxies. In Section 4 the surface brightness distribution function and the contribution of LSB galaxies to the mass density of the local Universe are discussed. Bivariate distribution functions of various galaxy parameters are presented in Section 5. Finally, in Section 6 we summarize the conclusions. Throughout this paper we use $H_0 = 100\,h_{100}$ km s^{-1} Mpc^{-1} for calculating distance dependent quantities.

2 THE DATA

The sample of galaxies used here to measure distribution functions of optical luminosity and central surface brightness is selected in the 21-cm line, and it is therefore free from selection effects related to optical surface brightness. The sample is the result of the Arecibo H I Strip Survey (AHISS), a blind extragalactic H I survey consisting of two strips of constant declination, together covering approximately 65 square degrees of sky over a depth of $cz = 7500$ km s^{-1}. The limiting column density for the central 3-arcmin wide strip (corresponding to the main beam of the Arecibo Telescope) was $\approx 10^{18}$ cm^{-2} (5σ) per resolution element of 16 km s^{-1} for gas filling the telescope beam. This sensitivity is unmatched by any other blind H I survey to date. Low-resolution 21-cm aperture synthesis observations of the AHISS sample of 66 galaxies have been obtained with the NRAO Very Large Array (VLA). Details of the Arecibo survey and the VLA observations are described by Sorar (1994) and Zwaan et al. (1997).

Optical observations were confined to sources at Galactic latitudes $|b| > 10°$ to avoid severe Galactic extinction and confusion of foreground stars. This reduces the total number of accessible sources to 61. The optical data were obtained at the Isaac Newton Telescope of the Observatorio del Roqué de los Muchachos on the island of La Palma, Spain. The data collection was spread over four observing runs during the period 1995 October through to 1997 March. Images were recorded at the Prime Focus camera with a thinned Tektronix 1024^2 pixel CCD. The Tektronix CCD has 24-μm pixels, which give an image scale of 0.59 arcsec per pixel at prime focus. All images were taken through a standard Harris B filter. Flat-fields were taken in the twilight, and the residual background variations after flatfielding are typically <1 per cent of the sky level. The photometric calibration was done by observing standard stars at several airmasses each night, and is accurate to 0.13 mag.

Total galaxy magnitudes were determined using aperture photometry on the reduced images. Correct aperture sizes were found using a curve-of-growth algorithm: aperture photometry was performed at a series of aperture radii, increasing in 1-arcsec steps, until the integrated magnitudes levelled out at an asymptotic maximum. The first radius at which this maximum (brightest) integrated magnitude was reached was then chosen as the correct aperture size. Central surface brightnesses and disc scalelengths were determined by fitting exponential disc models to the azimuthally averaged radial surface brightness profiles. The centres of the galaxies were usually taken to be the maximum of the light distribution. Strong central concentrations were excluded from the exponential fits. The data for galaxy A44 turned out to be unusable, which leaves us with a total number of 60 galaxies for our analysis.

We have chosen to apply the internal extinction correction proposed by Tully et al. (1998), which is a function of absolute magnitude. The extinction correction can be written as $A^{\rm i} = \gamma \log(a/b)$, where $\gamma = -0.35(15.1 + M_B^{\rm b,i})$. Because for our data set the central surface brightness is well-correlated with absolute luminosity, the extinction correction implies a low correction for LSB galaxies and a higher correction for high surface brightness (HSB) galaxies. Galactic extinction corrections have been applied using the reddening maps of Burstein & Heiles (1982) and assuming that $A(B) = 4.1E(B - V)$.

3 LUMINOSITY FUNCTIONS

The luminosity function (LF) of galaxies is defined as the number of galaxies Mpc^{-3} in a luminosity interval dM centred at magnitude M. The interval dM is generally taken to be 1 mag. The most used parametrization of the luminosity function is the Schechter (1976) function, defined by

$$\phi(M)\,{\rm d}M = 0.4 \ln 10 \phi^* [10^{0.4(M^*-M)}]^{1+\alpha} \times \exp[-10^{0.4(M^*-M)}]\,{\rm d}M, \quad (1)$$

where α is the faint-end slope, ϕ^* is the normalization factor and M^* is the characteristic absolute magnitude that defines the boundary between the exponential and power-law part.

3.1 Methods

Many different galaxy luminosity function estimators can be found in the literature. In Zwaan et al. (1997) we discuss different luminosity function estimators and conclude that the $\Sigma(1/V_{\rm max})$ method is the preferred way to determine mass functions and

luminosity functions for our sample. For this sample, we demonstrated that the determination of the H I mass function with the $\Sigma(1/V_{\rm max})$ method is not very sensitive to density fluctuations as a result of large-scale structure. The $\Sigma(1/V_{\rm max})$ method consists of summing the reciprocals of the volumes corresponding to the maximum distances at which galaxies could be seen and still remain within the sample. Summing these values per bin in H I mass or absolute magnitude immediately gives the binned H I mass function or optical luminosity function. The advantages of the $\Sigma(1/V_{\rm max})$ method are that it is automatically normalized and non-parametric; it recovers the amplitude and the shape of the luminosity function simultaneously, without using the Schechter function as an assumption about the intrinsic shape. An overview of the different galaxy luminosity function estimators is given by Willmer (1997), who tests the validity of different methods by means of Monte Carlo simulations. Careful examination of his tables shows that the $\Sigma(1/V_{\rm max})$ method (with binning in magnitudes) recovers the input luminosity function satisfactorily, and as equally well as the more conventional parameterized maximum likelihood method (Sandage, Tammann & Yahil 1979) or the Stepwise Maximum Likelihood Method (SWLM, Efstathiou, Ellis & Peterson 1988). Supported by this, we choose to apply the $\Sigma(1/V_{\rm max})$ method to evaluate the optical luminosity function. The details of the determination of the values of $V_{\rm max}$ are described in Zwaan et al. (1997) and will not be repeated here. Note that the values of $V_{\rm max}$ are derived from the original Arecibo H I survey parameters and are independent from the optical data.

3.2 Results

The resulting luminosity function $\phi(M_B)$ is shown in Fig. 1 as solid dots with 1σ error bars. The data are binned per 1.5 mag in order to obtain a reasonable number of galaxies per bin, but scaled in such a way that ϕ represents number densities per magnitude bins. Furthermore, the data are multiplied by a factor of 66/60 to account for the galaxies for which no optical information is available. To enable direct comparison with published luminosity functions, we choose to use the absolute magnitudes uncorrected for opacity effects in the galactic disc (see Leroy & Portilla 1998 for a discussion on the influence of optical depth effects on the shape of the luminosity function). The line indicates the best-fitting Schechter function which is determined by minimising χ^2 for the expected number of galaxies per bin. The uncertainties in the best fit are indicated in the inset that shows the 1σ and 2σ error contours of the χ^2 fit for α and M^* fitted jointly. As is usually the case in these fits, the parameters α and M^* are strongly correlated in the sense that steeper faint end slopes imply brighter values of M^*. The best-fitting Schechter parameters are found to be $\alpha = -1.03^{+0.25}_{-0.15}$, $M^* = -19.38^{+1.02}_{-0.62} + 5\log h_{100}$ mag and $\phi^* = (1.15 \pm 0.40) \times 10^{-2} h_{100}^{-3}\,{\rm Mpc}^{-3}$, where the quoted errors are 1σ one-parameter uncertainties. The uncertainties given here are solely the result of counting statistics, and therefore may understate the true uncertainties. Measurement errors in the parameters that define $V_{\rm max}$ and measurement errors in M_B also contribute to the uncertainties, but these are relatively small compared to the Poisson errors for this small sample.

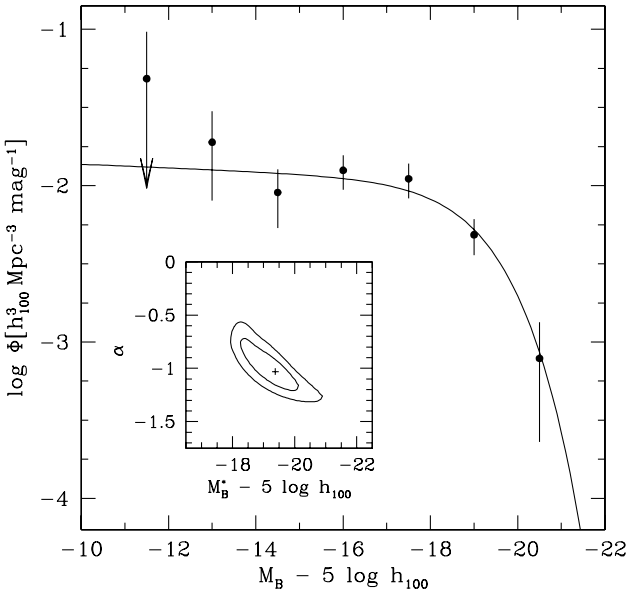

Figure 1. Luminosity function for H I selected galaxies. The points were determined using the $V_{\rm max}$ method, the error bars are 1σ uncertainties from Poisson statistics. The line is the best-fitting Schechter function with parameters: $\alpha = -1.03^{+0.25}_{-0.15}$, $M^* = -19.38^{+1.02}_{-0.62} + 5\log h_{100}$ mag and $\phi^* = (1.15 \pm 0.40) \times 10^{-2} h_{100}^{-3}\,{\rm Mpc}^{-3}$. The inset shows the 1σ and 2σ joint two-parameter confidence levels for α and M^*.

The parameterization in the form of a Schechter function is a satisfactory representation of luminosity function of the AHISS galaxies. However, because of the small number of galaxies in the low-luminosity bins, the value of the faint-end slope α is poorly constrained. Especially for magnitudes fainter than $M_B = -14$, the slope of the LF is almost unconstrained. There is no need for a modification of the LF, such as the Schechter function plus a power law, as proposed by Sprayberry et al. (1997) for his sample of LSB galaxies, although our present sample does not rule out this extra component. We note that our measured LF parameters are in excellent agreement with those from a preliminary analysis of the HIPASS survey (Marquarding 2000).

3.3 Comparison with optical determinations of the LF

It is interesting to compare the luminosity function for H I selected galaxies to luminosity functions of optically selected galaxies. Recently, there has been much interest in steep faint-end slopes of the luminosity function, and the galaxies responsible for this steep part (i) are found to be of late morphological type (e.g. Marzke et al. 1998), (ii) show strong emission lines indicative of active star formation (e.g. Zucca et al. 1997), and (iii) have blue colours (Lin et al. 1999). These are the types of galaxies that are expected to contain high fractions of H I, and therefore should be represented in the AHISS sample.

A vast number of luminosity functions based on optical redshift surveys is available in the literature. All these surveys contain typically a few 1000 galaxies. When making a comparison with our luminosity function for H I selected galaxies, we will concentrate on those studies which have made a specific distinction between late and early type galaxies, or star forming and quiescent galaxies. We consider: the Stromlo-APM redshift survey (APM, Loveday et al. 1992), the Center for Astrophysics redshift survey (CfA, Marzke et al. 1994), the ESO Slice Project (ESP, Zucca at al. 1997), the Las Campanas Redshift Survey (LCRS, Lin et al. 1996), the Autofib Redshift Survey (ARS, Heyl et al. 1997), the Second Southern Sky Redshift Survey (SSRS2, Marzke et al. 1998), the CNOC Field Galaxy Redshift Survey (CNOC2, Lin et al. 1999) and preliminary results from the 2dF survey (Folkes et al. 1999).

Table 1. Comparison of luminosity functions for late-type galaxies.

Sample	Selection	α	$M^* - 5\log h_{100}$	ϕ^{*a}	$\rho_L{}^b$
AHISS	H I selected	−1.03	−19.38	11.5	10.3 ± 2.0
APM (Loveday et al. 1992)	Sp/Irr	−0.80	−19.16	10	6.7
CfA (Marzke et al. 1994)	Sa-Sb	−0.58	−18.93[c]	8.7	8.9
	Sc-Sd	−0.96	−19.02[c]	4.4	
	Sm-Im	−1.87	−19.00[c]	0.6	
ESP (Zucca et al. 1997)	Emission lines	−1.40	−19.23	10	11.4
LCRS (Lin et al. 1997)	$3727W_\lambda \geq 5$ Å	−0.90	−18.93[d]	13	7.7
Autofib (Heyl et al. 1997)	Sab	−0.99	−19.76	2.19	8.4
	Sbc	−1.25	−19.16	2.80	
	Scd	−1.37	−18.96	3.01	
	Sdm	−1.36	−18.76	0.50	
SSRS2 (Marzke et al. 1998)	Spirals	−1.11	−19.43	8.0	9.2
	Irr/Pec	−1.81	−19.78	0.2	
CNOC2 (Lin et al. 1999)[e]	Intermediate type	−0.53	−18.97	9.0	11.1
	Late type	−1.23	−19.07	7.2	
2dF (Folkes et al. 1999)	Sab	−0.86	−19.44	3.9	14.0
	Sbc	−0.99	−19.14	5.3	
	Scd	−1.21	−18.76	6.5	
	Sdm-Im	−1.73	−18.78	2.1	

[a] Units are $10^{-3}\,h_{100}^3\,\mathrm{Mpc}^{-3}$.
[b] Units are $10^7\,h_{100}\,\mathrm{L}_\odot^B\,\mathrm{Mpc}^{-3}$.
[c] $B - M_Z = -0.21$.
[d] $B - R = 1.1$.
[e] Values extrapolated to $z = 0$.

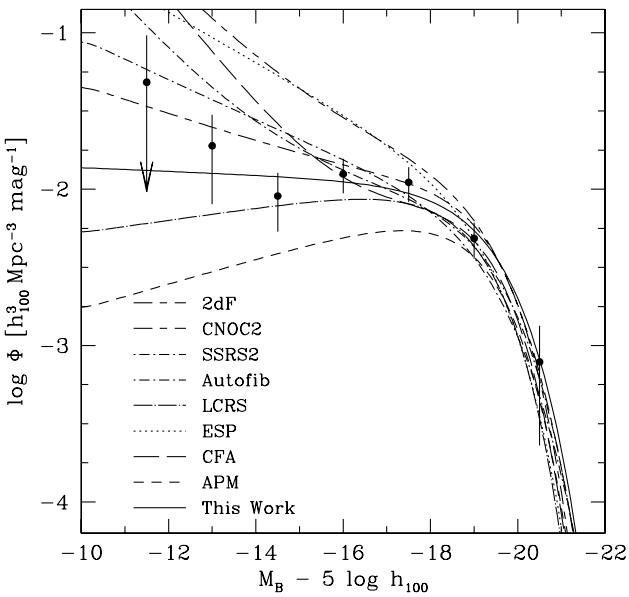

Figure 2. Luminosity functions for late-type galaxies. The points are the same as in Fig. 1. The lines show the luminosity functions from several recent redshift surveys. The details are given in Table 1. Some of these are the summations of several luminosity functions for different types.

Table 1 summarizes the Schechter parameters of 'late-type' luminosity functions of these surveys. In Fig. 2 these functions are represented, together with our measured points and the best-fitting Schechter function. The functions have been transformed to the B filter using the conversions $M_B = M_Z - 0.45$ for the CfA, $b - r = 1.1$ for the LCRS, and $M_B - M_{bJ} = 0.24$, and all functions are recalculated for $H_0 = 100\,h_{100}\,\mathrm{km\,s^{-1}\,Mpc^{-1}}$.

The direct comparison of these luminosity functions is rather naive for a number of reasons. First, different optical wavebands have been used in the selection of these galaxies. This effect can be corrected for by applying a magnitude correction, but this is most certainly a oversimplification of the problem. The use of different wavebands does not only have an influence on the luminosity of the selected galaxies but surely also on the morphological classifications. Secondly, the separation between late- and early-type galaxies has been made in different ways for each sample. In the CfA sample, a detailed separation between morphological types has been made on the basis of the appearances of the galaxies on the Palomar Sky Survey. Also, the SSRS2 and the APM samples have been classified by visual inspection. The CNOC2 data is split into different populations using colour information of the galaxies. For the 2dF and Autofib surveys spectral information has been used to make the classifications. The selection criteria for the ESP and the LCRS samples has been the occurrence of emission lines in the spectra. In the LCRS sample a distinction has been made on basis of the criterion of [O II] $3727W_\lambda \geq 5$ Å, in the EPS sample the selection was simply based on the detection the [O II] line.

With these restrictions in mind, we can compare the different luminosity functions for optically selected galaxies with those for H I selected galaxies. What is particularly striking is that the values of the faint-end slope span a wide range from −0.80 for the APM survey to ∼−1.50 for the ESP and 2dF surveys. Even for surveys that use comparable methods for classifying their different galaxy population, the differences in the faint-end slope can be large. Evidently, the shape of the luminosity distribution of late-type galaxies is still ill-constrained. On the other hand, the normalization and the value that defines the knee are quite similar for all surveys; all functions cross approximately the same point at $M_B \approx -19 + 5\log h_{100}$. The luminosity function for the AHISS falls in between those of the optical samples. We therefore conclude that our estimate of the luminosity function is in good agreement with that of optically selected samples. Furthermore, there is no new population selected by H I surveys that adds significantly to the galaxy populations identified through optical surveys.

3.4 Luminosity density of gas-rich galaxies

A more fundamental parameter is the luminosity density, the integrated light from the whole population of galaxies. As is discussed by Lilly et al. (1996), this parameter is in principle less dependent on the details of galaxy evolution than the luminosity function. The integral luminosity density of late-type galaxies can be determined by integrating the Schechter luminosity function weighted by luminosity, which gives $j_B = \phi^* L_B^* \Gamma(2+\alpha)$, where Γ is the Euler gamma function. The values of j_B for late-type galaxies as determined by the different optical surveys are given in the last column of Table 1. It is remarkable that all values of j_B are within $\sim 1.5\sigma$ from the value determined from the AHISS. A notable exception is the 2dF survey, which finds a value 60 per cent higher than the mean of the other surveys. Folkes et al. (1999) note that the 2dF results are preliminary, and that the corrections for completeness, clustering and Malmquist-bias have not been applied yet. It remains to be seen whether the final 2dF results will remain in excess of the AHISS estimate of j_B. A preliminary result from the SDSS (Blanton et al. 2001) has a substantially higher optical luminosity density than other recent surveys, but this increase appears to arise in their photometric evaluation of the luminosity of each galaxy, rather than an increase in the number density of objects.

The mean value of j_B of all the optically selected late-type galaxy samples is $9.7 \times 10^7\, h_{100}\, \mathrm{L}_\odot^B\, \mathrm{Mpc}^{-3}$, while that for the AHISS sample is $(10.3 \pm 2.0) \times 10^7\, h_{100}\, \mathrm{L}_\odot^B\, \mathrm{Mpc}^{-3}$. This latter value translates to $j_B = (3.4 \pm 0.7) \times 10^{19}\, h_{100}^{-2}\, \mathrm{W\,Hz^{-1}\,Mpc^{-3}}$, using the conversion of Lilly et al. (1996). This is approximately 50 per cent of the integral luminosity density of the local Universe as measured by the most recent optical redshift surveys using isophotal magnitudes (Folkes et al. 1999, Blanton et al. 2001). Blanton et al. (2001) find that j_B increases significantly if extrapolated magnitudes are used.

3.5 Luminosity and H I mass distributions for different morphological types

A more detailed view of the relative importance of different morphological types to the H I and luminosity density can be made be transforming luminosity functions into H I mass functions, assuming correlations between H I mass and optical luminosity. Rao & Briggs (1993) used this method to determine the H I mass function and $\Omega_{\rm HI}$ based on the luminosity functions available at that time. They showed that by adopting the relation $\log M_{\rm HI} = a - bM_B$ between H I mass and optical luminosity, the H I mass function can be written as

$$\Theta(M_{\rm HI})\,\mathrm{d}(M_{\rm HI}) = \frac{0.4}{b}\,\phi^* \left(\frac{M_{\rm HI}}{M_{\rm HI}^*}\right)^{(\alpha+1)\frac{0.4}{b}-1} \times \exp\,-\left(\frac{M_{\rm HI}}{M_{\rm HI}^*}\right)^{\frac{0.4}{b}} \mathrm{d}\left(\frac{M_{\rm HI}}{M_{\rm HI}^*}\right), \qquad (2)$$

where $\log M_{\rm HI}^* = a - bM_B^*$, and α and ϕ^* are the Schechter parameters of the luminosity functions.

Here we update the calculations by Rao & Briggs (1993) with more recent luminosity function parameters, and test if the results are in agreement with our measurements. For completeness, we present all possible ways of plotting the number density, the H I density and the luminosity density as a function of absolute magnitude and H I mass. We adopt the Marzke et al. (1998) luminosity functions for different morphological types, and we fit linear regression lines to $M_{\rm HI}$ versus M_B taken from the Nearby Galaxy Catalog (Tully 1988) to find the values of a and b.

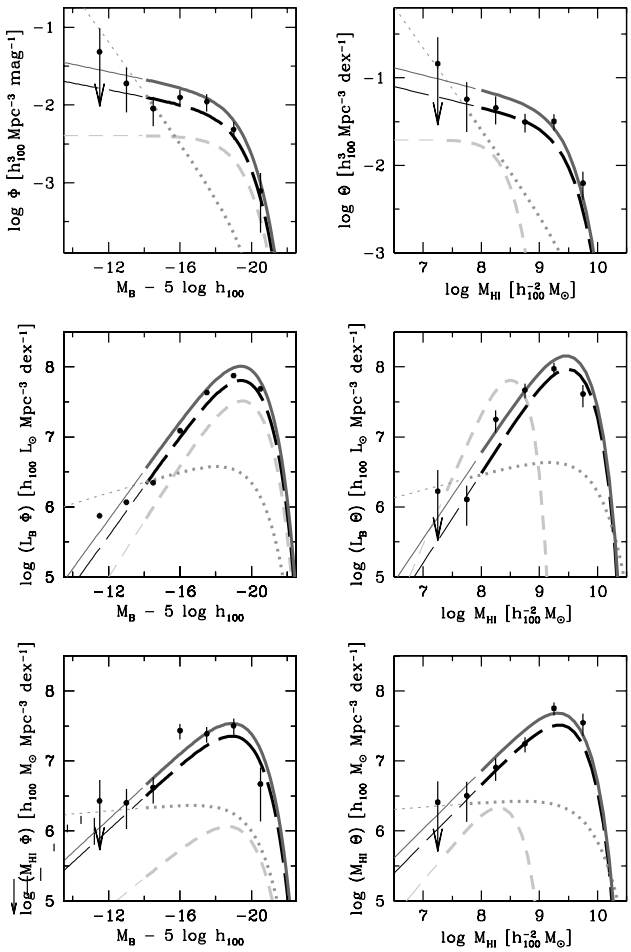

Figure 3. Luminosity and H I density functions for different morphological types. The points are from the AHISS and are the result of the $1/V_{\rm max}$ method. The lines are converted functions for different morphological types, using Marzke et al. (1998) luminosity functions, and H I to M_B relations from the Nearby Galaxy Catalog (Tully 1988). The solid grey lines are for all galaxy types, the black dashed lines for spirals, the grey dashed lines are for E and S0, and the grey dotted lines are for Irr/Pec. The thin parts of each line are extrapolations beyond the confidence levels set by Marzke et al. (1998). *Upper left panel*: Luminosity function. *Upper right panel*: H I mass function. *Middle left panel*: Luminosity density as a function of M_B. *Middle right panel*: Luminosity density as a function of $M_{\rm HI}$. *Lower left panel*: H I density as a function of M_B. *Lower right panel*: H I density as a function of $M_{\rm HI}$.

Fig. 3 shows the results. The solid grey lines are for all galaxy types, the black dashed lines are for spirals, the grey dashed lines are for E and S0 types, and the grey dotted line is for Irr/Pec types. The thin parts of each line are extrapolations beyond the confidence levels set by Marzke et al. (1998). The solid points plus error bars are different representations of the AHISS data. The results are basically the same as those found by Rao & Briggs (1993). We show here that the optical luminosity functions, combined with conversion factors from M_B to $M_{\rm HI}$, give excellent fits to our data. The H I density distribution matches the converted luminosity functions for all galaxy types summed, and the luminosity distribution is fitted satisfactorily with spiral and

irregular population. It is no surprise that the luminosity density from ellipticals exceeds the measured values from the AHISS, because these objects are not selected by H I surveys. This is especially clear in the middle right panel.

The integral H I density can be determined from a optical luminosity functions via

$$\rho_{\rm HI} = \int_{-\infty}^{+\infty} \Phi(L) M_{\rm HI}\, {\rm d}L = \phi^* 10^{a-bM^*} \Gamma(1+\alpha+2.5b). \qquad (3)$$

If we apply this to our adopted luminosity functions, we find that spirals make up 62 per cent of the H I gas density, Irr and Pec types contribute 35 per cent, and E and S0 types only contribute 3 per cent. Natarajan & Pettini (1997) apply this same method to measurements of the luminosity function at higher redshift in order to chart the evolution of the cosmic gas content between $z = 1$ and $z = 0$. The viability of this result is unclear because the amount of evolution of the $M_{\rm HI}L$ ratio of galaxies is presently unknown. Future deep H I surveys at redshifts $z > 0$ are required to constrain the $M_{\rm HI}/L$ evolution.

4 CONTRIBUTION OF LSB GALAXIES TO THE COSMIC MASS BUDGET

More than two decades after the seminal paper by Disney (1976), who defined the potential selection effects against LSB galaxies, the debate on the cosmological significance of LSB galaxies is still open. The AHISS sample, which is not biased by the sky background, makes a valuable contribution to the discussion of the cosmological significance of LSB galaxies.

4.1 The surface brightness distribution function

The bottom panel of Fig. 4 shows a histogram of the distribution of *B*-band surface brightnesses for the AHISS galaxies. These surface brightnesses are corrected for dust extinction following the formalism described by Tully et al. (1998). The unshaded histogram shows the distribution for the full set of AHISS galaxies, and the grey histograms show the distribution for the subset of AHISS galaxies with inclinations $i \leq 75°$ for which the corrections to face-on values are modest. The galaxies with high inclinations ($i > 75°$) do not appear, from their optical images, to be very low surface brightness: they often exhibit bright central condensations and strong dust lanes, both features not normally found in extreme LSB galaxies (see McGaugh, Schombert & Bothun 1995). It therefore seems possible that the true face-on surface brightness of these discs is brighter than those given by either the Tully et al. (1998) prescription or the assumption that the discs are fully transparent.

The top panel of Fig. 4 shows the volume-corrected surface brightness distribution function of AHISS galaxies. This function is determined by summing values of $1/V_{\rm max}$ per 1-mag bins of surface brightness. The error bars indicate 68 per cent confidence levels and are determined from 100 bootstrap re-sample realizations of the data. The hollow symbols show the distribution for the complete set of AHISS galaxies, and the solid symbols are limited to those AHISS galaxies with $i \leq 75°$. Note that the distribution function resembles the one found by Sprayberry et al. (1996) based on the APM survey.

4.2 A cut-off in surface brightness?

As Fig. 4 shows, the AHISS detected no galaxies with reliably

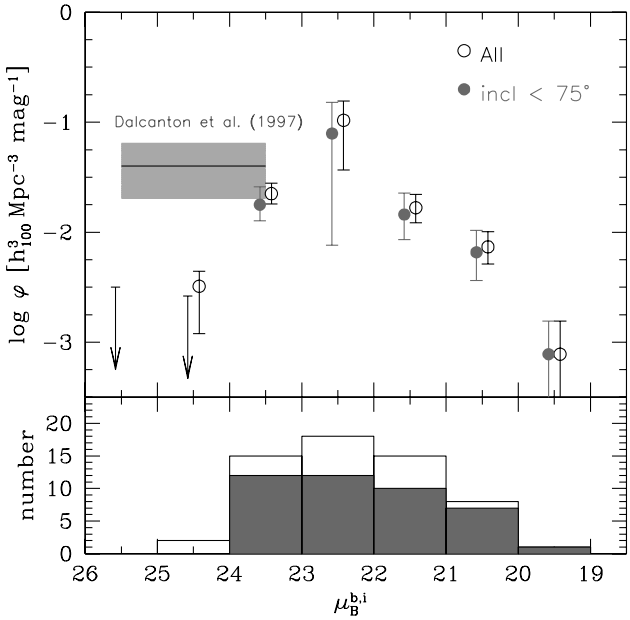

Figure 4. *Bottom panel*: Distribution of surface brightnesses in the AHISS sample. The grey histogram is for those galaxies with $i \leq 75°$ and is embedded in the histogram for all galaxies. *Top panel*: volume corrected distribution of surface brightnesses. The open and solid symbols have the same meaning as in the bottom panel. For clarity, the points are slightly offset horizontally. Errorbars indicate 68 per cent confidence levels. Arrows denote 95 per cent confidence upper limits. The space density of optically selected LSB galaxies determined by Dalcanton et al. (1997b) is indicated by a light grey box, and corresponds to 90 per cent confidence levels.

determined face-on central surface brightnesses fainter than $\mu_B^{\rm b,i} = 24\,{\rm mag\,arcsec^{-2}}$. Even among the highly inclined galaxies with large (and possibly unreliable) corrections to face-on values, there are no galaxies with $\mu_B \gtrsim 25\,{\rm mag\,arcsec^{-2}}$. The statistical significance of these results depends on the assumptions we make about the detectability of very LSB systems. We can make an estimate by calculating the average value of $V_{\rm max}$ for the different surface brightness bins. We find that $V_{\rm max}$ is mildly correlated with $\mu_B^{\rm b,i}$: dimmer galaxies can on average be detected over smaller volumes. This correlation arises because decreasing surface brightness correlates with decreasing total H I mass, and the sample selection is based on H I flux. If we extrapolate the $\mu_B^{\rm b,i} - V_{\rm max}$ correlation to the surface brightness bins in which we have no detections, we find that $\langle V_{\rm max}\rangle$ would be $1150\,h_{100}^{-3}\,{\rm Mpc}^3$ for the 24–25 mag arcsec^{-2} bin, and $950\,h_{100}^{-3}\,{\rm Mpc}^3$ for the 25–26 mag arcsec^{-2} bin. The probability p_k of finding k objects when the mean is n, is given by the Poisson distribution: $p_k = {\rm e}^{-n} n^k/k!$. The mean number of detected objects mag^{-1} is given by $\varphi(\mu)V_{\rm max}(\mu)$, where $\varphi(\mu)$ is the space density of objects as a function of surface brightness. Hence, the probability of finding zero sources in one bin is $p_0 = {\rm e}^{-\varphi(\mu)V_{\rm max}(\mu)}$. A 95 per cent confidence upper limit to $\varphi(\mu)$ can now be expressed as $\varphi(\mu) = -\ln(0.05)/V_{\rm max}(\mu)$. This equation is used for the upper limits, which are indicated by arrows in Fig. 4.

This absence of extreme LSB galaxies suggests two things. First, the space density of massive, gas-rich, extremely LSB discs such as Malin 1 (Bothun et al. 1987) must be low, as previously shown by, for, Briggs (1990, 1997), Driver & Cross (2000) and Blanton et al. (2001). Such a disc would have been easily detectable to the limit of $7500\,{\rm km\,s^{-1}}$ of the AHISS, so they must be intrinsically less common on average than 1 per $1000\,h_{100}^{-3}\,{\rm Mpc}^3$ (95 per cent

confidence level, using the Poisson statistics). Secondly, optical surveys for LSB galaxies (Sprayberry et al. 1996; Dalcanton et al. 1997b; O'Neil et al. 1997) systematically find galaxies at lower surface brightnesses than $\mu(0) = 24\,\mathrm{mag\,arcsec^{-2}}$, so there must be some reason why the present H I survey fails to detect any.

One possibility is that such galaxies have detectable amounts of neutral hydrogen but are extremely rare, so that it would not be expected to find one in the AHISS search volume. Apart from a few special objects like Malin 1, this seems unlikely because optical surveys find these objects in significant numbers despite the relatively small volume limits imposed by optical surface brightness selection effects (McGaugh 1996). Specifically, Dalcanton et al. (1997b) find that the number density of galaxies with *V*-band central surface brightnesses in the range $23 < \mu < 25\,\mathrm{mag\,arcsec^{-2}}$ is $0.08^{+0.05}_{-0.04}\,h^3_{100}\,\mathrm{Mpc^{-3}}$ comparable to the number density of normal galaxies. For reference, we have indicated this estimate with a shaded box in Fig. 4, where we have adopted $B - V = 0.5$, a typical value for LSB galaxies (de Blok, van der Hulst & Bothun 1995).

The other possibility is that a significant number of galaxies exist in the AHISS search volume with optical surface brightnesses $\mu(0) > 24\,\mathrm{mag\,arcsec^{-2}}$, but that they do not contain enough H I to be detected by the AHISS. This seems considerably more likely, as there are two ways such a population could come to exist. first, these very low density systems could have formed a first generation of stars and then either lost most of their remaining gas through supernova-driven winds (Babul & Rees 1992; Babul & Ferguson 1996) or consumed all their gas in vigorous star formation and since then faded to become LSB discs (Bell et al. 1999). Secondly, like the outskirts of normal spiral galaxies, LSB discs have low H I surface densities (de Blok, McGaugh & van der Hulst 1996), and as such, they are subject to ionization by the extragalactic ultraviolet (UV) background that produces the sharp cut-offs seen at the edges of normal spirals, for column densities below $10^{19.5}\,\mathrm{cm^{-2}}$ (e.g. Maloney 1993; Corbelli & Salpeter 1993; Dove & Shull 1994). Thus, much of the gas in LSB discs should become ionized, and thus be undetectable in 21-cm surveys. This is consistent with the finding that no AHISS galaxies were found with average H I column densities lower than $\langle N_{\rm HI}\rangle > 10^{19.7}\,\mathrm{cm^{-2}}$ (Zwaan et al. 1997). The average limiting column density of the AHISS was $\approx 10^{18}\,\mathrm{cm^{-2}}$ (5σ) per $16\,\mathrm{km\,s^{-1}}$. Of course, for many galaxies in the AHISS sample this number is not the minimal detectable H I column density averaged over the gas disc. Not all detected galaxies fill the beam of the Arecibo Telescope, and the velocity width of all detections is larger than $16\,\mathrm{km\,s^{-1}}$. A typical AHISS galaxy fills 50 per cent of the beam and has a velocity width of $160\,\mathrm{km\,s^{-1}}$. With optimal smoothing applied, the minimal detectable column density of such a galaxy would be $10^{18.8}\,\mathrm{cm^{-2}}$, still approximately an order of magnitude lower than the reported cut-off of $10^{19.7}\,\mathrm{cm^{-2}}$ in Zwaan et al. (1997). Moreover, the detection limit of very large galaxies or gas clouds that do fill the beam and have a similar velocity width of $160\,\mathrm{km\,s^{-1}}$ would be even lower, approximately $10^{18.5}\,\mathrm{cm^{-2}}$. None of these extended, low column density systems were detected.

At present there is insufficient data to distinguish between the two proposed hypotheses. Currently available studies of the stellar compositions of LSB galaxies (McGaugh & Bothun 1994; de Blok et al. 1995; Bell et al. 1999, 2000) have concluded that gas-rich LSBs form stars slowly and continuously and therefore have fairly young stellar populations. Judging from their colours, the newly identified class of red LSB galaxies (O'Neil, Bothun & Schombert 2000) are consistent with a scenario in which they are simply a fading, passively evolving population (Bell et al. 1999). However, O'Neil et al. (2000) report that some of these galaxies have high values of $M_{\rm HI}L$, but they also note that 60 per cent of their LSB galaxy sample that was followed-up with Arecibo is *undetected* in H I, in sharp contrast to the high success rate in earlier LSB samples (e.g. Schneider et al. 1990). Moreover, a cross-correlation of the tables in O'Neil et al. (1997) and O'Neil et al. (2000) shows that the global $V - I$ colours of the undetected galaxies are on average 0.3 mag redder than the galaxies in which H I was found.

Multicolour photometry of galaxies with $\mu_B > 24.0\,\mathrm{mag\,arcsec^{-2}}$, in combination with deep Hα imaging and deep 21-cm observations, should show whether the lowest surface brightness galaxies are consistent with a fading, passively evolving population.

4.3 The LSB contribution to the neutral gas density

To address the problem of the cosmological significance of gas-rich LSB galaxies in a meaningful way, an LSB galaxy should be well-defined. In the literature, different authors adopt different definitions for the critical surface brightness that separates galaxies into the 'normal' and LSB classes. The critical value ranges from $21.65\,\mathrm{mag\,arcsec^{-2}}$ (the 'Freeman value') to $23.5\,\mathrm{mag\,arcsec^{-2}}$. In the remainder of this paper we define an LSB galaxy as a galaxy with de-projected *B*-band central surface brightness $>23.0\,\mathrm{mag\,arcsec^{-2}}$. This limits the LSB galaxies to those that are $\sim 4\sigma$ dimmer than the Freeman value.

The cumulative distribution of H I density among AHISS galaxies of different surface brightness is presented in the top panel of Fig. 5. The H I density distribution can be fitted satisfactorily with a Gaussian distribution. There is no fundamental physical motivation for using a Gaussian to parameterize the distribution function, but Dalcanton, Spergel & Summers (1997a) note that a galaxy formation scenario based on a log-normal distribution of the spin parameter λ produces a (nearly) Gaussian function of luminosity density versus surface brightness (see also de Jong & Lacey 2000). The inset in Fig. 5 gives 1σ and 2σ confidence ellipses for the Gaussian fits, the horizontal axis shows the centre of the distribution and the vertical axis shows the dispersion (1σ). The actual fitting was done on the binned data, not on the cumulative distribution.

The H I mass density of the local Universe is dominated by galaxies dimmer than the Freeman (1970) value of $21.7\,\mathrm{mag\,arcsec^{-2}}$. The peak of the differential distribution is at $22.0\,\mathrm{mag\,arcsec^{-2}}$ and the width is $1.0\,\mathrm{mag\,arcsec^{-2}}$. Low surface brightness galaxies contribute a minor fraction to the H I density, galaxies fainter than $23.0\,\mathrm{mag\,arcsec^{-2}}$ make up 18^{+6}_{-5} per cent of the H I mass density in the local Universe (the quoted errors have been determined using bootstrap re-sampling and mark the 68 per cent confidence levels).

4.4 The LSB contribution to the luminosity density

The lower panel of Fig. 5 shows the cumulative distribution of luminosity density against surface brightnesses. The peak of the differential distribution is at $21.2\,\mathrm{mag\,arcsec^{-2}}$ and the 1σ dispersion is $1.0\,\mathrm{mag\,arcsec^{-2}}$. This implies that while most of the H I resides in galaxies dimmer than the Freeman value, most of the light in gas-holding galaxies in the local Universe is in galaxies 0.5 mag brighter than the Freeman value. The contribution of LSB galaxies is insignificant; galaxies with $\mu_B^{\rm b,i} > 23\,\mathrm{mag\,arcsec^{-2}}$ constitute no more than 5 ± 2 per cent to the luminosity density.

We stress that this result only holds for gas-rich LSB galaxies.

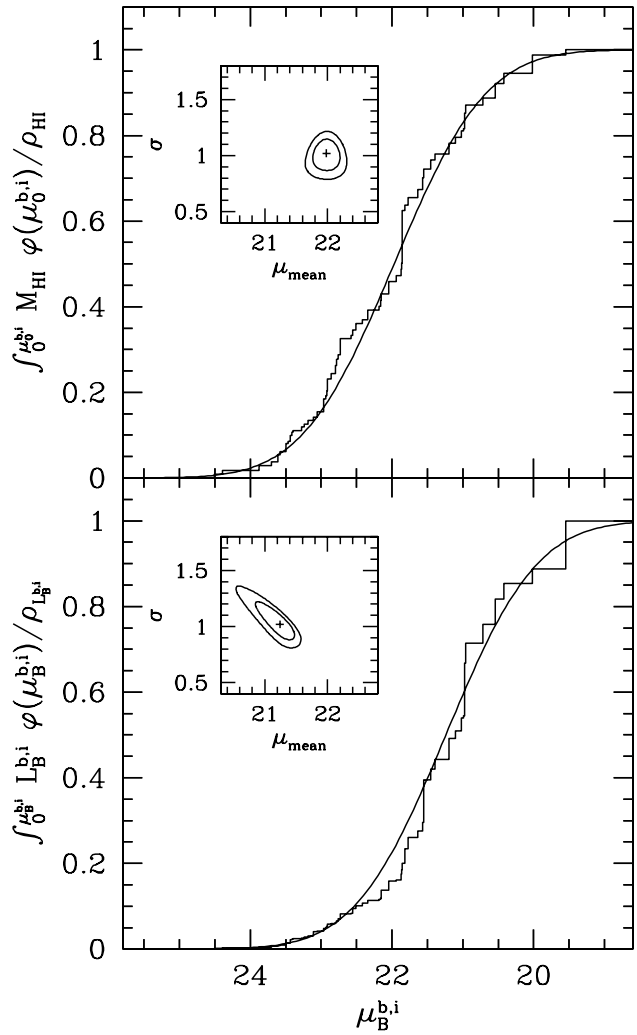

Figure 5. Cumulative distributions of H I mass density (top panel) and luminosity density (bottom panel) as a function of central surface brightness for the AHISS sample. The lines show Gaussian fits. The 1σ confidence levels on the two jointly fitted parameters μ and σ, the mean and the width of the Gaussian, are shown in the inset. The H I density of the local Universe is dominated by galaxies with *B*-band central surface brightness of 22.0 mag arcsec^{-2}, the luminosity density is dominated by 21.2 mag arcsec^{-2} galaxies for this H I selected sample.

The contribution of gas-free LSB galaxies is unconstrained by our survey. Sprayberry et al. (1997) conclude that optically selected LSB galaxies contribute about 30 per cent to the field galaxy luminosity density, a result very consistent with ours, as their definition of an LSB galaxy is $\mu_B > 22.0$ mag arcsec^{-2}. De Jong & Lacey (2000) find that the luminosity density of optically selected galaxies is dominated by $\mu_I \sim 19.3$ mag arcsec^{-2}, which compares to 21.0 mag arcsec^{-2} in the *B*-band (using their value of $B-I=1.7$). They estimate that approximately 4 per cent of the luminosity density is provided by galaxies with $\mu_B^{b,i} > 22.75$ mag arcsec^{-2}. Driver (1999) defines a volume limited subsample of 47 galaxies at $0.3 < z < 0.5$ from the Hubble Deep Field and derives that LSB galaxies (mean surface brightness within the effective radius > 21.7 mag arcsec^{-2}) contribute 7 ± 4 per cent to the luminosity density. All these results are in good agreement with our estimates. This fact implies that if a population of very LSB, gas-free LSB galaxies exists (as was discussed in Section 4.2), their contribution to the luminosity density must be negligible.

4.5 The LSB contribution to $\Omega_{\rm matter}$

The contribution of LSB galaxies to the total mass budget of the local Universe is a longstanding question. The calculation critically depends on the assumptions one makes on the dependence of the dynamical *ML* on central surface brightness. A zeroth order approximation is to assume that *ML* is equal for all galaxies, independent of central surface brightness. This assumption follows naturally from the observation that surface brightness is not a parameter in the Tully–Fisher relation (Sprayberry et al. 1995; Zwaan et al. 1995; Verheijen 1997). Moreover, Verheijen (1997) shows that it is possible to use one model for the dark matter halo to fit the rotation curves of three galaxies, all at equal positions in the Tully–Fisher relation, but with different surface brightnesses. In the terminology of McGaugh & de Blok (1998), this invariant *ML* would be the 'same halo hypothesis'. It is consistent with the idea that all galaxies of equal luminosity form in the same mass halo, but the angular momentum of an LSB disc is higher, which causes the disc to be less centrally concentrated (Dalcanton et al. 1997a). Combined with the result on the luminosity density from Section 4.4, this assumption leads to the conclusion that $\rho_{\rm M}$(LSB) is 5 per cent of the total ρ_M (i.e. equal to the contribution to the luminosity density).

Van den Bosch & Dalcanton (2000) show that their semi-analytical galaxy models are consistent with $M/L \propto \Sigma^{-1/2}$ (Zwaan et al. 1995), where Σ is the central surface brightness in linear units. *M*/*L* ratios are calculated via $M \propto DV^2$, where *V* is the maximum rotational velocity and *D* is a characteristic size of the dark halo, which is assumed to be directly proportional to the scalelength of the optical disc. If we, like Driver (1999), adopt this relation for *M*/*L* we find that the LSB contribution to ρ_M rises to 11^{+4}_{-3} per cent. If we apply the calculations of $M \propto DV^2$ directly to our AHISS data set, we find $\rho_{\rm M}({\rm LSB}) = 10^{+4}_{-3}$ per cent. Both values are in excellent agreement with the 12 ± 6 per cent that Driver finds.

At present it is unclear what the true dependence of the dynamical *ML* on optical surface brightness is. Clearly, high-precision measurements of rotation curves of LSB systems are needed (see Swaters, Madore & Trewhella 2000; van den Bosch & Swaters 2001; van den Bosch et al. 2000). At the moment we adopt as a conservative estimate that gas-rich LSB galaxies contribute no more than 11 per cent to ρ_M, the dynamical mass contained in galaxies.

5 BIVARIATE DISTRIBUTIONS

A more detailed view of the distribution of baryons among galaxies of different sizes and brightnesses can be obtained by calculating bivariate distribution functions. The importance of this way of looking at galaxy parameters is stressed by van der Kruit (1987, 1989), de Jong (1996) and most recently by de Jong & Lacey (2000), who study 10^3 galaxies with types Sb to Sdm. First, the bivariate distribution function is a important constraint for galaxy formation theories, as any theory should not only produce the integrated luminosity function (and integrated distribution functions of other structural parameters), but also higher dimensional distribution functions. Secondly, bivariate distribution functions help to clarify the selection effects that influence the determination of (e.g.) the luminosity function.

The aim of the present work is (i) to test whether an H I selected galaxy sample yields qualitatively the same bivariate distribution function, and (ii) to extend the bivariate distribution functions to

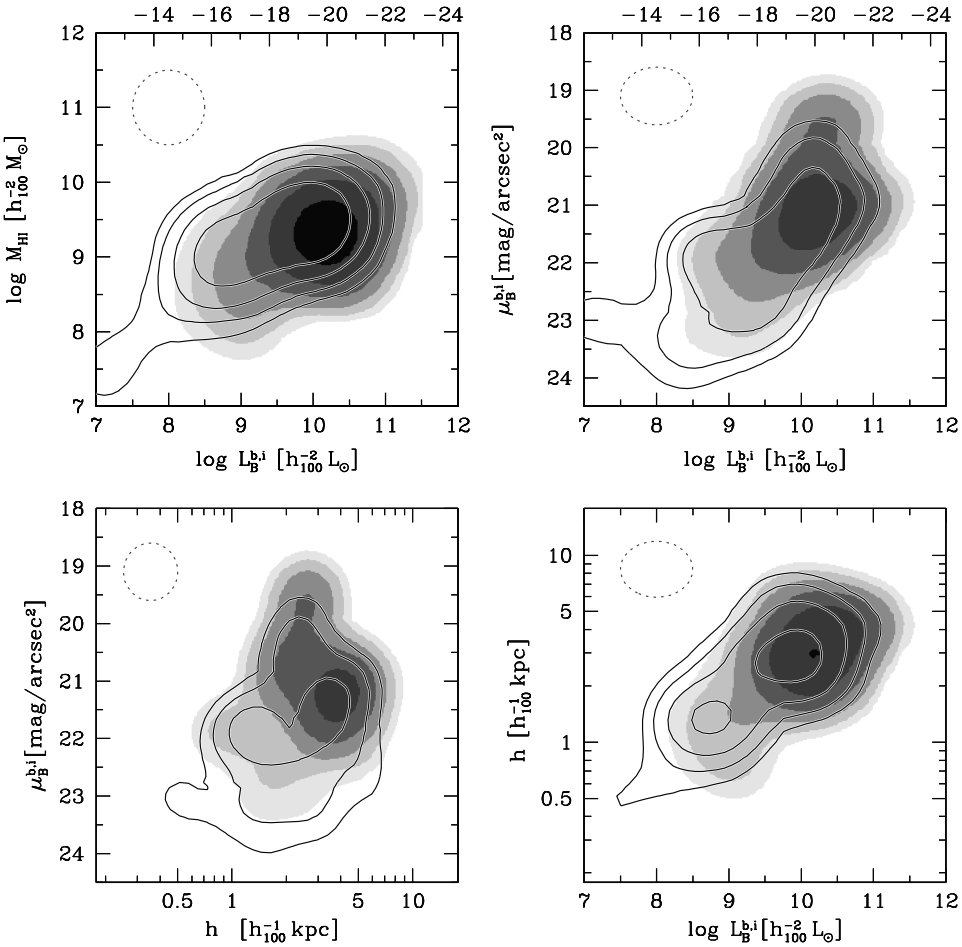

Figure 6. Bivariate distribution of luminosity density (grey-scales) and H I density (contours) for H I selected galaxies in the ($L_B^{b,i}$, M_{HI})-plane (*top left*), the ($L_B^{b,i}$, $\mu_B^{b,i}$) − plane (*top right*), the (h, $\mu_B^{b,i}$) − plane (*lower left*), and the ($L_B^{b,i}$, h) − plane (*lower right*). Grey-scales correspond to ($10^{6.5}$, $10^{6.75}$, $10^{7.0}$, …) $h_{100}\,L_\odot\,Mpc^{-3}$, contours to ($10^{6.25}$, $10^{6.5}$, $10^{6.75}$, …) $h_{100}\,M_\odot\,Mpc^{-3}$. The densities are per decade for $L_B^{b,i}$ and M_{HI}, per 0.3 dex for h and per mag for $\mu_B^{b,i}$. The dashed ellipses in the upper right corners of each panel indicate the FWHM of the Gaussian smoothing filter that has been applied to the data.

the distribution of H I properties. The sample we study here is small, and, as is discussed by de Jong & Lacey (1999) and Minchin (1999), at least 500–1000 galaxies are required to avoid problems with small number statistics. We only intend to make qualitative comparisons and care should be taken with the interpretation of the results. We also stress that the sample that we use here might be biased against galaxies with very low values of M_{HI}/L, just like optical samples are biased to those with high values of M_{HI}/L.

5.1 Results

In Fig. 6 we present bivariate distributions of several fundamental parameters. Our aim is to show the distribution of H I mass density and luminosity density as a function of galaxy luminosity, gas mass, size and surface brightness.

The figures are calculated by distributing values of M_{HI}/V_{max} and $L_B^{b,i}/V_{max}$ over a fine grid with 0.1-dex resolution for M_{HI} and $L_B^{b,i}$, 0.1-mag resolution for central surface brightness $\mu_B^{b,i}$ and 0.05-dex resolution for disc scalelength h. Next, the images were smoothed with a Gaussian filter, of which the full width at half-maximum (FWHM) values are indicated by the dashed ellipses in the upper left corners of each panel. The H I density distributions are shown as contours, the luminosity density distribution as grey-scales. Steps in intensity are in logarithmic intervals of 0.25 dex.

The first thing to notice is that the general trends are the same for the gas density and the luminosity density, but the maximum of the gas density is shifted towards less luminous, lower surface brightness galaxies. The second point is that the luminosity density is more strongly concentrated towards large, luminous HSB galaxies, whereas the H I density is more widely distributed.

What is obvious from the top right panel is that both the luminosity and the H I mass distribution are strongly dependent on optical surface brightness in the sense that both functions are shifted towards fainter absolute magnitudes for lower surface brightness galaxies. This fact was also observed by de Jong (1996), and the peak of the distribution, at $M_B^{b,i} = -20 + 5\log h_{100}$ and $\mu_B^{b,i} = 21$ mag arcsec^{-2} agrees well with his determination. The same trend is observed by Cross et al. (2001) who present a bivariate distribution function based on a preliminary subsample of 5×10^4 galaxies from the 2dF survey and by Blanton et al. (2001) who use a sample of 10^4 galaxies from the SDSS commissioning data.

A similar effect can be seen in the lower right panel: the luminosity and the H I mass distribution are shifted towards fainter absolute magnitudes for smaller galaxies. This correlation has been studied in detail by de Jong & Lacey (2000), who discuss the predictions of hierarchical galaxy formation theories and conclude that the observed distribution is in qualitative agreement with theory, but the distribution in disc size is narrower than predicted.

6 CONCLUSIONS

We have presented several volume corrected distribution functions for galaxies that have been selected in the H I 21-cm line. The conclusions are as follows.

(i) The luminosity function of the H I selected galaxies is in agreement with other determinations based on late-type or star-forming galaxies. The integral luminosity density of gas-rich, late-type or star-forming galaxies is well determined and equals $j_B = (3.4 \pm 0.7) \times 10^{19} h_{100}^{-2}\,\mathrm{W\,Hz^{-1}\,Mpc^{-3}}$. This is approximately 50 per cent of the integral luminosity density of the local Universe.

(ii) The contribution of low surface brightness (LSB) galaxies to the integral luminosity density and H I density is modest, 5 and 18 per cent, respectively. This in good agreement with calculation based on optically selected galaxies. The fraction of Ω_{matter} that resides in LSB galaxies is at present not well determined, but is probably less than 11 per cent.

(iii) We observe a lower limit to the surface brightness of gas-rich galaxies: no galaxies were found with de-projected central surface brightness $> 24.0\,\mathrm{mag\,arcsec^{-2}}$ in the B band. It will be interesting to test whether this result stands up with future large H I surveys, such as the HIPASS survey (Staveley-Smith et al. 1996).

(iv) Bivariate distributions of various fundamental galaxy parameters show that the H I density in the local Universe is more diffusely spread over galaxies with different size, surface brightness, and luminosity than the luminosity density. The luminosity density is concentrated towards bright, large, high surface brightness discs.

ACKNOWLEDGMENTS

We thank L. Staveley-Smith, R. Webster and B. Koribalski for helpful comments. The Isaac Newton Telescope is operated by the Royal Greenwich Observatory in the Spanish Observatorio del Roque de los Muchachos of the Instituto de Astrofisica de Canarias. The National Radio Astronomy Observatory is a facility of the National Science Foundation operated under cooperative agreement by Associated Universities, Inc. The Arecibo Observatory is part of the National Astronomy and Ionosphere Center, which is operated by Cornell University under a cooperative agreement with the National Science Foundation. The National Radio Astronomy Observatory is a facility of the National Science Foundation operated under cooperative agreement by Associated Universities, Inc.

REFERENCES

Babul A., Ferguson H. C., 1996, ApJ, 458, 100
Babul A., Rees M. J., 1992, MNRAS, 255, 346
Bell E. F., de Blok W. J. G., 2000, MNRAS, 311, 668
Bell E. F., Bower R. G., de Jong R. S., Hereld M., Rauscher B. J., 1999, MNRAS, 302, L55
Bell E. F., Barnaby D., Bower R. G., de Jong R. S., Harper D. A., Hereld M., Loewenstein R. F., Rauscher B. J., 2000, MNRAS, 312
Blanton M. R. et al., 2001, AJ, 121, 2358
Bothun G. D., Impey C. D., Malin D. F., Mould J. R., 1987, AJ, 94, 23
Briggs F. H., 1990, AJ, 100, 999
Briggs F. H., 1997, ApJ, 484, 618
Broadhurst T. J., Ellis R. S., Shanks T., 1988, MNRAS, 235, 827
Burstein D., Heiles C., 1982, AJ, 87, 1165
Cole S., Lacey C. G., Baugh C. M., Frenk C. S., 2000, MNRAS, 319, 168
Corbelli E., Salpeter E. E., 1993, ApJ, 419, 104
Cross N. et al., 2001, MNRAS, 324, 825
Dalcanton J. J., Spergel D. N., Summers F. J., 1997a, ApJ, 482, 659
Dalcanton J. J., Spergel D. N., Gunn J. E., Schmidt M., Schneider D. P., 1997b, AJ, 114, 635
de Blok W. J. G., van der Hulst J. M., Bothun G. D., 1995, MNRAS, 274, 235
de Blok W. J. G., McGaugh S. S., van der Hulst J. M., 1996, MNRAS, 283, 18
de Jong R. S., 1996, A&A, 313, 45
de Jong R. S., Lacey C., 1999, in Impey C., Phillipps S., eds, ASP Conf. Ser. Vol. 170, The Low Surface Brightness Universe. Astron. Soc. Pac., San Francisco, p. 52
de Jong R. S., Lacey C., 2000, ApJ, 545, 781
Disney M. J., 1976, Nat, 263, 573
Disney M. J., Phillipps S., 1987, Nat, 329, 203
Dove J. B., Shull J. M., 1994, ApJ, 423, 196
Driver S. P., 1999, ApJ, 526, L69
Driver S. P., Phillipps S., 1996, ApJ, 469, 529
Driver S. P., Cross N., 2000, in Kraan-Korteweg R. C., Hennning P. A., Andernach H., eds, ASP Conf. Ser. Vol. 218, Mapping the Hidden Universe. Astron. Soc. Pac., San Francisco, p. 309
Efstathiou G., Ellis R. S., Peterson B. A., 1988, MNRAS, 231, 479
Ellis R. S., 1997, ARA&A, 35, 389
Folkes S. et al., 1999, MNRAS, 308, 159
Freeman K. C., 1970, ApJ, 160, 811
Heyl J., Colless M., Ellis R. S., Broadhurst T., 1997, ApJ, 489, 67
Impey C. D., Sprayberry D., Irwin M. J., Bothun G. D., 1996, ApJS, 105, 209
Koo D. C., Kron R. G., 1992, ARA&A, 30, 613
Leroy P., Portilla M., 1998, A&A, 329, 840
Lilly S. J., Le Fevre O., Hammer F., Crampton D., 1996, ApJ, 460, 1
Lin H., Kirshner R. P., Shectman S. A., Landy S. D., Oemler A., Tucker D. L., Schechter P. L., 1996, ApJ, 464, 60
Lin H., Yee H. K. C., Carlberg R. G., Morris S. L., Sawicki M., Patton D. R., Wirth G., Shepherd C. W., 1999, ApJ, 518, 533
Loveday J., Peterson B. A., Efstathiou G., Maddox S. J., 1992, ApJ, 390, 338
Maloney P., 1993, ApJ, 414, 41
Marquarding M., 2000, MSc thesis, Univ. Melbourne
Marzke R. O., Geller M. J., Huchra J. P., Corwin H. G., 1994, AJ, 108, 437
Marzke R. O., da Costa L. N., Pellegrini P. S., Willmer C. N. A., Geller M. J., 1998, ApJ, 503, 617
McGaugh S. S., 1996, MNRAS, 280, 337
McGaugh S. S., Bothun G. D., 1994, AJ, 107, 530
McGaugh S. S., de Blok W. J. G., 499,1998 41
McGaugh S. S., Schombert J. M., Bothun G. D., 1995, AJ, 109, 2019
Minchin R. F., 1999, Pub. Ast. Soc. Aus., 16, 12
Natarajan P., Pettini M., 1997, MNRAS, 291, 28
O'Neil K., Bothun G. D., 2000, ApJ, 529, 811
O'Neil K., Bothun G. D., Schombert J., Cornell M. E., Impey C. D., 1997, AJ, 114, 2448
O'Neil K., Bothun G. D., Schombert J., 2000, AJ, 119, 136
Rao S., Briggs F. H., 1993, ApJ, 419, 515
Ratcliffe A., Shanks T., Parker Q. A., Fong R., 1998, MNRAS, 293, 197
Sandage A., Tammann G. A., Yahil A., 1979, ApJ, 232, 352
Schechter P., 1976, ApJ, 203, 297
Schneider S. E., Thuan T. X., Magri C., Wadiak J. E., 1990, ApJS, 72, 245
Sorar E., 1994, PhD thesis, Univ. Edinburgh
Sprayberry D., Bernstein G. M., Impey C. D., Bothun G. D., 1995, ApJ, 438, 72
Sprayberry D., Impey C. D., Irwin M. J., 1996, ApJ, 463, 535
Sprayberry D., Impey C. D., Irwin M. J., Bothun G. D., 1997, ApJ, 482, 104
Staveley-Smith L. et al., 1996, Pub. Ast. Soc. Aus., 13, 243
Swaters R. A., Madore B. F., Trewhella M., 2000, ApJ, 531, L107
Tully R. B., 1988, Nearby Galaxies Catalog. Cambridge Univ. Press, Cambridge
Tully R. B., Verheijen M. A. W., 1997, ApJ, 484, 145

Tully R. B., Pierce M. J., Huang J., Saunders W., Verheijen M. A. W., Witchalls P. L., 1998, AJ, 115, 2264
van den Bosch F. C., Dalcanton J. J., 2000, ApJ, 534, 146
van den Bosch F. C., Swaters R. A., 2001, MNRAS, 325, 1017
van den Bosch F. C., Robertson B. E., Dalcanton J. J., de Blok W. J. G., 2000, AJ, 119, 1579
van der Kruit P. C., 1987, A&A, 173, 59
van der Kruit P. C., 1989, in Gilmore G., King I., van der Kruit P., eds, The Milky Way as a Galaxy. Geneva Observatory, Switzerland, p. 257
Verheijen M. A. W., 1997, PhD thesis, Univ. Groningen
Willmer C. N. A., 1997, AJ, 114, 898
Zucca E. et al., 1997, A&A, 326, 477
Zwaan M. A., van der Hulst J. M., de Blok W. J. G., McGaugh S. S., 1995, MNRAS, 273, L35
Zwaan M. A., Briggs F. H., Sprayberry D., Sorar E., 1997, ApJ, 490, 173

This paper has been typeset from a TEX/LATEX file prepared by the author.